Microporous and Mesoporous Materials 236 (2016) 158–166

Contents lists available at ScienceDirect

Microporous and Mesoporous Materials

journal homepage: www.elsevier.com/locate/micromeso

Optically transparent silver-loaded mesoporous thin film coating with long-lasting antibacterial activity

Paolo Nicolas Catalano [a, *], Magdalena Pezzoni [b], Cristina Costa [b], Galo Juan de Avila Arturo Soler-Illia [c], Martin Gonzalo Bellino [a, **], Martin Federico Desimone [d, ***]

[a] Departamento de Micro y Nanotecnología, Instituto de Nanociencia y Nanotecnología-Comisión Nacional de Energía Atómica, CONICET, Av. General Paz 1499, B1650KNA San Martín, Argentina
[b] Departamento de Radiobiología, Comisión Nacional de Energía Atómica, Av. General Paz 1499, B1650KNA San Martín, Argentina
[c] Instituto de Nanosistemas, Universidad Nacional de General San Martín, Av. 25 de Mayo 1021, 1650 San Martín, Argentina
[d] Universidad de Buenos Aires. IQUIMEFA - CONICET, Facultad de Farmacia y Bioquímica, Junín 956 Piso 3. (1113), Ciudad Autónoma de Buenos Aires, Argentina

ARTICLE INFO

Article history:
Received 4 July 2016
Received in revised form
18 August 2016
Accepted 29 August 2016
Available online 31 August 2016

Keywords:
Antibacterial
Transparent coating
Mesoporous thin film
Silver

ABSTRACT

Infectious diseases caused by microorganisms affect millions of people worldwide. In an effort to prevent infections induced by bacteria, a variety of antibacterial coatings have been designed. In this sense, the possibility to combine broad-range bactericidal agents such as silver and chemically and mechanically stable matrices such as mesoporous oxide thin films has been encouraging. In this study, titania–silica bilayer mesoporous thin film (MTF) coatings have been produced and loaded with silver species, and their bactericidal efficiency against *Pseudomonas aeruginosa* and *Staphylococcus* aureus was assessed over time. In this sense, coatings loaded with silver ions (MTF + Ag^+) were analyzed in comparison with coatings confining silver nanoparticles (MTF + AgNP). EDS analysis revealed that both types of MTF coatings were loaded with high amounts of silver (MTF + Ag^+ = 25%; MTF + AgNP = 34%). MTF + Ag^+ showed extremely high bactericidal efficiency (percent reduction of 99.5 to >99.999) against both strains along 10 cycles of use, comparable to that observed with MTF + AgNP. Interestingly, silver release from both types of coatings was similar over the same testing period. However, contrary to MTF + AgNP, MTF + Ag^+ have shown absolute optical transparency. This is relevant for any type of coating, as conservation of optical properties of the material surface where they are intended to be applied, is highly desirable. Moreover, the maximum silver ion sorption capacity of film coatings was 3 μg cm^{-2} and MTF + Ag^+ were still loaded with silver after 10 cycles of use which indicates that the bactericidal effect could be extended beyond. These results spotlight the potentiality of MTF + Ag^+ as antibacterial coatings for any ceramic and/or metallic surface with no alteration of optical and mechanical properties.

1. Introduction

Infectious diseases induced by microorganisms like bacteria, fungi and viruses are still one of the greatest health problems worldwide. Intensive research has been devoted to drug development for combating those infections. Other efforts were directed to strengthen prevention, particularly by designing antibacterial coatings with natural and synthetic organic compounds and/or inorganic substances. Among these, antibacterial properties of silver are well known [1,2], and are still largely exploited in many consumer products and medical devices. Silver is nowadays applied in antimicrobial packaging films [3,4], textiles and sprays to protect from odor-generating microorganisms [5,6], in cosmetics [7], in wound dressing [8,9] and in medical implants and instruments [10,11].

The broad-range bactericidal effect of metallic silver is ascribed to the release of silver ions (Ag^+) from its surface [12]. The antibacterial effect of this ion is due to interactions with thiol and

* Corresponding author.
** Corresponding author.
*** Corresponding author.
E-mail addresses: catalano@cnea.gov.ar (P.N. Catalano), mbellino@cnea.gov.ar (M.G. Bellino), desimone@ffyb.uba.ar (M.F. Desimone).

http://dx.doi.org/10.1016/j.micromeso.2016.08.034
1387-1811/

amino groups of proteins and with nucleic acids [2,13–15] leading to inactivation and loss of replication ability, respectively. Silver cations also induce cell membrane damage and production of reactive oxygen species that may alter lipids and DNA [16–18]. Considering the current high level of bacterial resistance against antibiotics, silver is used for disinfection as metal coatings, silver salts and nanoparticles. However, low stability and poor long-term antibacterial efficiency may limit its practical applications. For this reason, different materials with slow silver ions release rate and long-term antibacterial activity are required.

Silver-based coatings are aimed at reducing or even preventing microbial colonization and the formation of so-called biofilms, bacteria self-synthesized shelters which are highly difficult to eradicate [19,20]. Metallic silver coatings have been applied in permanent implants such as megaendoprostheses used in reconstruction after removal of bone tumors [11] and have been incorporated in biocompatible coatings, such as hydroxyapatite [21,22] to reduce surgical site infection in orthopedic and dental implants. However, in order to gain more control over the ion release, focus has recently shift from bulk silver to nanostructured coatings [23]. Nanomaterials offer remarkable advantages in antibacterial applications owing to their high surface area and unique physicochemical properties, which depend on their size and shape [24–26]. In this sense, silver nanoparticles have found multiple applications and showed higher antibacterial efficiency than bulk silver materials [27–29].

Silver nanoparticles are frequently included in composite coatings offering flexible and tailorable structures, together with diverse methods for nanoparticle immobilization [30–34]. Combination of nanosilver and organic matrices is profitable as it facilitates nanoparticle synthesis, processing and immobilization, and minimizes nanoparticle aggregation and uncontrollable release of silver ions [35,36]. Many of these antibacterial coatings have been based in organic polymers [9,37–39] or proteins [40,41], which present some limitations when chemical and mechanical stability are required. As an alternative, mesoporous oxide thin films (MTFs) offering high surface area and the possibility to be tailored in order to control the pore size, shape and interconnectivity, has been widely used to confine silver nanoparticles within the porous reservoirs, leading to an enhanced stability of the nanoparticles [42–45]. Particularly, bactericidal synergy under UV irradiation between photocatalytic titanium dioxide (TiO_2) MTFs and immobilized silver nanoparticles within this porous matrix was recently reported [43,45].

Although the application of MTFs with confined silver nanoparticles has been extensively investigated, nanosilver exhibits a strong absorption of visible light, significantly altering the optical quality of coatings based on MTFs which are originally transparent [46–48]. This is particularly critical for ceramic and/or metallic surfaces where their optical properties must be conserved owing to functional and/or esthetic reasons. Therefore, there is still a need to develop silver-based transparent antibacterial MTF coatings for surfaces which require conservation of their optical properties. Instead of using silver nanoparticles as reservoirs of silver ions, a solution can be achieved by using mesoporous systems as reservoirs through direct adsorption of silver ions.

In this study, titania-silica bilayer MTF coatings were used as nanostructured reservoirs for silver ions, and their antibacterial activity was assessed. The films were synthesized onto glass slides by combining the sol-gel and evaporation-induced self-assembly methods and subsequently incubated with silver nitrate solution to promote adsorption of silver ions on the mesoporous matrix. Optical properties, estimation of silver content, ion adsorption and release, and long-term antibacterial activity for Gram+ (*Staphylococcus aureus*)and Gram- (*Pseudomonas aeruginosa*) bacteria were evaluated in comparison with analogue films containing photodeposited silver nanoparticles within the mesoporous titania layer. Optically transparent MTF coatings loaded with silver ions exhibited long-lasting antibacterial activity comparable to the non-transparent MTF coatings with confined silver nanoparticles, spotlighting its potentiality as antibacterial coatings for any ceramic and/or metallic surface with no alteration of optical and mechanical properties.

2. Experimental

2.1. Synthesis and deposition of mesoporous layers

Standard microscope glass slides were thoroughly washed with neutral detergent (Extran®, Merck Millipore, Darmstadt, Germany), then sequentially rinsed with miliQ water, acetone and isopropanol, and finally dried under nitrogen flow. Titania-silica bilayer MTFs were prepared by sequential dip-coating (withdrawal rate of 2 mm s^{-1}) on the glass substrates at a relative humidity (RH) of 40–50% [49]. A first layer of mesoporous TiO_2 was deposited on the glass substrates, obtained from a $TiCl_4$/ethanol solution to which the organic template Pluronics F127 ($HO(CH_2CH_2O)_{106}(CH_2CH(CH_3)O)_{70}(CH_2CH_2O)_{106}OH$) (Sigma-Aldrich) and water were added. The final composition of the precursor solution was $TiCl_4$:ethanol:H_2O:F127 equal to 1:40:10:0.005 mol ratios. The substrates were dip-coated at 35 °C solution temperature. After deposition, the samples were placed in a 50% RH chamber for 24 h and subjected to a consolidation thermal treatment consisting of two successive stages of 24 h at 60 and 130 °C, followed by a final heat treatment at 200 °C for 2 h. Next, a second layer of mesoporous SiO_2 was deposited on top of the deposited TiO_2 layer. Tetraethyl orthosilicate (TEOS) (Sigma-Aldrich) was used as the inorganic precursor and PluronicsF127 was selected as the template. TEOS was prehydrolyzed by refluxing for 1 h in a water/ethanol solution; $[H_2O]/[Si] = 1$; $[EtOH]/[TEOS] = 5$. Surfactant, ethanol and acidic water were added to this prehydrolyzed solution in order to prepare the precursor solution with final composition TEOS:ethanol:H_2O (0.1 M HCl):F127 equal to 1:40:5:0.005 mol ratios. After this second deposition, the samples were introduced into a 50% RH chamber for 24 h and then thermally stabilized with two successive stages of 24 h at 60 °C and 130 °C. To stabilize the overall structure and to remove the organic template a final thermal treatment at 350 °C for 2 h (temperature ramp of 2 °C/min) was performed. Glass slides with deposited mesoporous bilayer were cut into sample pieces of 26 mm long and 20 mm wide (5.2 cm^2).

2.2. Silver ions adsorption and photodeposition of silver nanoparticles

Film samples were immersed in a 0.1 M $AgNO_3$ water-ethanol solution (1:1 vol ratio) for 10 min in the dark to optimize ion infiltration. Subsequently, samples were individually placed in a 60 mm plastic culture dish and 7 mL of the silver solution previously mentioned was added to each one so the film samples were completely immersed. One group of immersed samples was incubated for 60 min in the dark. Another group was placed 4 cm below a UV tube lamp (Yarlux, 15 W, emission peak at 355 nm) for 60 min. All the samples were then withdrawn from the silver solution and thoroughly rinsed with water and dried under nitrogen flow.

2.3. Film coatings characterization

Transmission electron microscopy (TEM) images of MTF coatings were obtained using a Phillips CM 200 electron microscope (Amsterdam, The Netherlands). Samples were obtained by

scratching the coatings from the substrate and deposit on carbon coated copper grids. Film thickness, porosity and pore size distribution values were obtained from environmental ellipsometric porosimetry (SOPRA GES5A; SOPRA, Inc.; Palo Alto, CA). Pore diameters were obtained from the pore size distribution function using a Kelvin model with a precision of ±0.5 nm using Winelli III software (SOPRA). Optical quality of the films was analyzed by UV–vis spectroscopy employing a Hewlett-Packard 8453 spectrophotometer (Palo Alto, CA) in transmission mode. Estimation of silver content within MTF coatings was determined by calculation of Ag:Ti mass fractions using quantitative energy-dispersive X-ray spectroscopy (EDS) microanalysis in scanning electron microscopy (SEM, Quanta 200, FEI, Hillsboro, OR). Silver ion release from film coatings to liquid medium was determined by successive 24 h-exposure of films to a fresh 350 μL-aliquot of water for 10 days. The fitting curve for the cumulative silver release was obtained using the following first-order kinetics equation:

$$M_t = M_0\left(1 - e^{-kt}\right)$$

where M_t is the accumulated silver mass released at any given time t, M_0 is the initial silver mass, k is the first-order rate constant.

Determination of silver ion adsorption isotherm was performed by exposing individual films to different concentrations of $AgNO_3$ and monitoring the remaining silver concentration after 60 min of incubation. The maximum adsorption capacity of film coatings Q ($\mu g\ cm^{-2}$), was determined using the following equation:

$$Q = \frac{V(Ci - Ce)}{A}$$

where Ci and Ce are the initial and equilibrium silver concentrations ($\mu g\ mL^{-1}$), V is the solution volume (mL) and A (cm^2) is the film area exposed to the silver solution. The fitting curve was obtained using Langmuir equation:

$$q_{eq} = \frac{q_m K_a C_{eq}}{1 + K_a C_{eq}}$$

where C_{eq} is the silver concentration in the equilibrium, K_a is the equilibrium constant and q_m is the maximum adsorption capacity. Langmuir model considers that the interaction between sorbate and sorbent is homogeneous, with homogeneous adsorption sites until the first monolayer is formed on the sorbent surface [50].

In all cases, silver in liquid media was quantified using an S2 Picofox total reflection X-ray fluorescence spectrometer (Bruker, Berlin, Germany).

2.4. Determination of antibacterial activity of film coatings

The bacteria used in this study were *Pseudomonas aeruginosa* (PAO1) and *Staphylococcus aureus* (ATCC 29213). These strains were routinely grown at 37 °C in Luria–Bertani (LB) broth (yeast extract, 5 g L^{-1}; NaCl, 10 g L^{-1} and triptone, 10 g L^{-1}); 15 g L^{-1}agar was added when solid medium was used. The antibacterial activity of MTF coatings loaded with silver ions or with silver nanoparticles was tested on *P. aeruginosa* and *S. aureus* following the standard methodology to characterize antibacterial coatings [51]. Sample surfaces were consecutively exposed for 10 cycles to 350 μL-inoculums with an average concentration of ca. 1×10^7 CFU mL^{-1}. Inoculums were prepared by 1/500 dilution in sterile saline solution of overnight cultures and were then spread on the surface of each sample in triplicate. Inoculated samples were incubated at 37 °C for 24 h in a humidified chamber to avoid evaporation. For each cycle, aliquots of cell suspensions were taken before (0 h) and after (24 h) exposure to MTF coatings; the neat suspension and 10-fold serial dilutions were plated onto LB solid medium. The plates were incubated at 37 °C for 24 h and the colonies were counted to assess cell viability. Control samples were MTF-coated glass slides that were not incubated with silver solution. Between cycles, all samples were sequentially washed with ethanol 70% and sterile water.

Antibacterial activity was calculated using two different parameters: percent reduction ($D\%$) and value of antimicrobial activity (R). $D\%$ was calculated from untreated MTF coatings − treated MTF coatings microbial count percentage ratio.

R was calculated according to JIS Z 2801:2000 [51]:

$$R = \log (B/C)$$

where B is the average number of viable bacteria on the untreated MTF coating after 24 h and C is the average number of viable bacteria on the treated MTF coatings, either loaded with silver ions or with silver nanoparticles, after 24 h.

2.5. Statistics

All quantitative results were obtained from triplicate samples. Data were expressed as mean ± SD. Statistical analysis was carried out using the two-way ANOVA and Bonferroni multiple comparisons post-test. A value of $p > 0.05$ was considered to be statistically significant.

3. Results and discussion

In this study, bactericidal efficiency of silver–loaded MTF coatings was assessed over time. Two different silver ion-releasing systems were evaluated: coatings loaded with silver ions and coatings with embedded silver nanoparticles (Scheme 1). For this purpose, titania-silica bilayer MTF composition was selected as basal structure. Owing to titania photoactivity, silver nanoparticles can be selectively confined in that mesoporous layer by *in situ* photoreduction of silver ions, leaving the upper silica mesoporous layer free of particles [52,53]. Silver nanoparticles have shown to directly attach to cell membrane surfaces inducing poration and their internalization. Further damage through nanoparticles interaction with intracellular proteins and DNA could be produced [54,55]. By using a titania-silica bilayer structure, bacterial suspensions were not directly exposed to silver nanoparticles but to silver ions that were gradually released from them. In this way, the bactericidal effect of these releasing ions could be exclusively evaluated. For adequate comparison, the same bilayer configuration was used for adsorbing silver ions without formation of silver nanoparticles. Both MTF coatings were characterized and their antibacterial properties over 10 cycles of use were determined.

Fig. 1 shows representative TEM images of the titania-silica mesoporous bilayer. These images show a top-view of superimposed layers, where the lower mesoporous titania layer is seen clearer and poked out from the upper mesoporous silica layer which is seen darker. As expected, incubation with silver ions did not introduce any significant modification on the bilayer structure when compared with previous results [56] (Fig. 1A). Whereas, Fig. 1B shows the presence of well-defined silver nanoparticles on the lower titania layer of MTF coatings that were exposed to UV radiation upon silver ion adsorption. Characterization of deposited MTF layers by environmental ellipsometric porosimetry revealed that mesoporous titania exhibited a uniform 10 nm pore size distribution, a porosity of 37% and a thickness of 160 nm. Upper mesoporous silica layer exhibited a uniform 9 nm pore size distribution, a porosity of 37% and a thickness of 80 nm. All these data

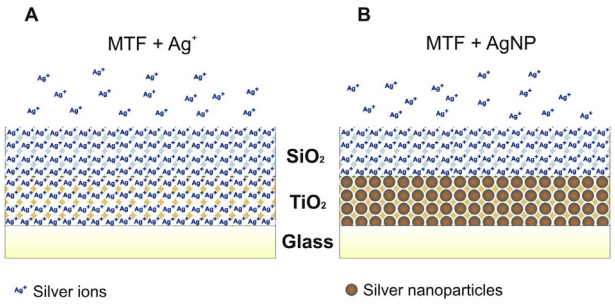

Scheme 1. Silver-loaded MTF coating systems evaluated in the study. (A) MTF coatings loaded with silver ions (MTF + Ag^+) showing Ag^+ adsorbing onto mesoporous silica and titania layers, and (B) MTF coatings loaded with silver nanoparticles (MTF + AgNP) showing confining of these particles in the lower mesoporous titania layer and Ag^+ adsorbing onto the upper mesoporous silica layer.

demonstrated the extremely high surface area of the coating which is less than 250 nm thick.

EDS analysis performed on mesoporous titania thin films confirms that they are composed mainly by titania and oxygen, although silicon was also detected due to the glass substrate employed for film deposition (Fig. 2A). After deposition of the silica layer the amount of silicon detected increased significantly (Fig. 2B and C), which is in close agreement with the superimposed bilayer structure of the coatings.

Estimation of silver content after incubation with silver solution and after photodeposition of silver nanoparticles by calculation of Ag:Ti mass fractions using EDS, demonstrated that both MTF coatings were able to load high amounts of silver (MTF coating + Ag^+ = 25%; MTF coating + AgNP = 34%) (Fig. 2B and C). Considering that the isoelectric point of mesoporous silica is ca. 2–3 [57,58], it is expected that silver ions would electrostatically adsorb onto the upper mesoporous silica layer, given that pH of the silver nitrate solution used for the coating preparation was 4.3. When considering the lower mesoporous titania layer, a priori, the situation would not be as clear as in the case of the mesoporous silica layer. Even though the reported isoelectric point for mesoporous titania is in the range of 5–6 [59,60], the value strongly depends on the crystalline structure and the nanoscale morphology [61], may extending this range to lower values. In fact, estimation of silver content by calculation of Ag:Ti mass fractions using EDS on mesoporous titania thin films (lower layer only) after incubation with silver solution, revealed that a significant amount of silver ions adsorbed onto the titania layer (18%) (Fig. 2A). Therefore, we propose that silver ions adsorb on both layers of the MTF coating (Scheme 1).

A key point for coatings is whether they may affect the optical properties of the material surface where they are intended to be applied. It is well known that silver nanoparticles exhibit a strong absorption of visible light and their inclusion could significantly alter the optical quality of coatings based on MTFs. Fig. 3 shows that

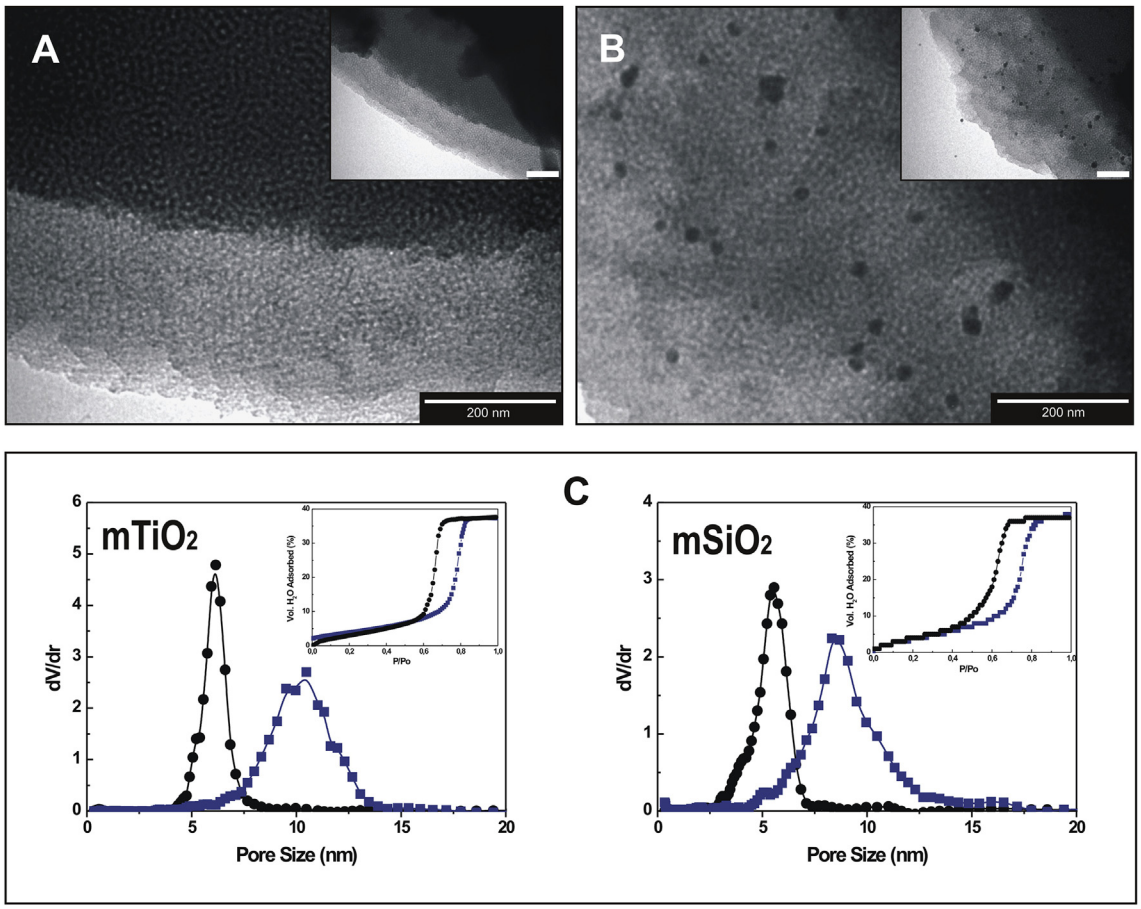

Fig. 1. TEM images showing the morphologies of bilayer thin films with adsorbed silver ions (A) and confined silver nanoparticles (B). Insets: Images on lower magnification for an enlarged view. Scale bar 200 nm. (C) Representative pore size distribution (blue line) and neck size distribution (black line) of mesoporous titania thin films (left) and mesoporous silica thin films (right) used in this study obtained by water adsorption–desorption isotherms at 298 K. (For interpretation of the references to colour in this figure legend, the reader is referred to the web version of this article.)

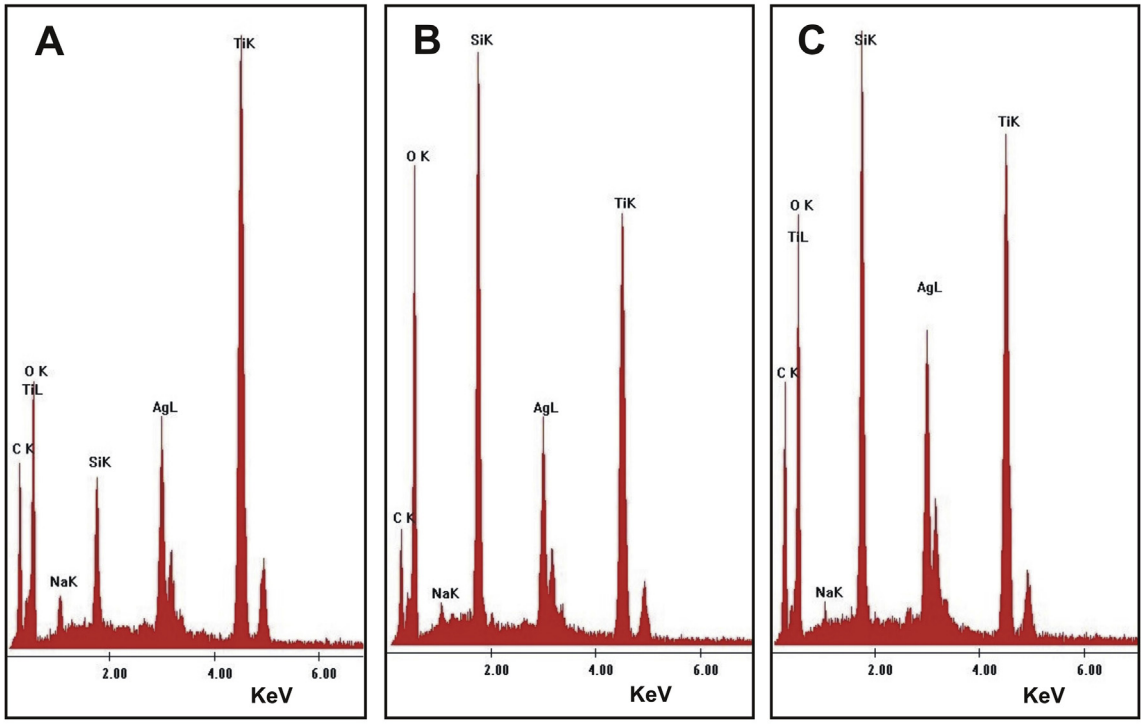

Fig. 2. Representative EDS spectra of titania thin films on a glass substrate incubated with $AgNO_3$ 0.1 M solution for 60 min (A), MTF coatings loaded with silver ions (B) and MTF coatings with confined silver nanoparticles (C).

MTF coatings with confined silver nanoparticles absorb light in almost the entire visible wavelength range. On the contrary, MTF coatings with adsorbed silver ions showed no absorption of visible light, similar to non-treated MTF coatings, demonstrating that they remained optically transparent after ion adsorption.

Considering that both MTF coating systems were loaded with silver, either silver ions alone or a combination of silver ions and silver nanoparticles, the antibacterial activity of coatings over time was analyzed. For this purpose, two prototypical bacterial strains were selected: *Pseudomonas aeruginosa* and *Staphylococcus aureus*. *P. aeruginosa* is a gram-negative rod-shaped bacterium used as model in biofilm and corrosion studies and *S. aureus* is a gram-positive coccal bacterium used as model in bacterial suspension studies. Both microorganisms are also important opportunistic pathogens in humans. In order to evaluate the antibacterial activity of MTF coatings, after exposing them to bacteria, changes in cell viability were evaluated by counting colony forming units (CFU). In all cases a high concentration of bacteria was used as inoculum to emulate the worst case scenario, inasmuch as survival of a lower concentration of bacteria would be inhibited in the same or greater extent. When analyzing the antibacterial activity of MTF coatings against *P. aeruginosa*, both MTF coating systems showed an antibacterial efficiency >99.999 at least until the tenth cycle of use (Fig. 4A). The bactericidal effect of these coatings was also analyzed against *S. aureus*. In this case, the percent reduction of viable microorganisms exposed over 24 h to MTF coatings with embedded silver nanoparticles was>99.999 along 10 cycles of use. Meanwhile, MTF coatings loaded with silver ions showed an antibacterial efficiency >99.999% up to the sixth cycle of use and maintained an excellent performance, superior to 99.5%, even after the tenth cycle of use (Fig. 4B). In addition, it is worth to mention that the value of antimicrobial activity (R) obtained by the JIS Z 2801:2000 testing method shall not be less than 2.0 for the surface antimicrobial efficacy of antimicrobial products. On one hand, there were no differences in antimicrobial activity against *Pseudomonas aeruginosa* between MTF coatings loaded with silver ions or silver nanoparticles. Moreover the R value was higher than 6 in all cycles of use; these values are three times higher than the minimum established by the standard norm to recognize the antimicrobial efficacy of a material, highlighting the successful antimicrobial activity of the MTF coatings (Table 1). On the other hand, a different situation was observed in the case of the Gram + bacteria

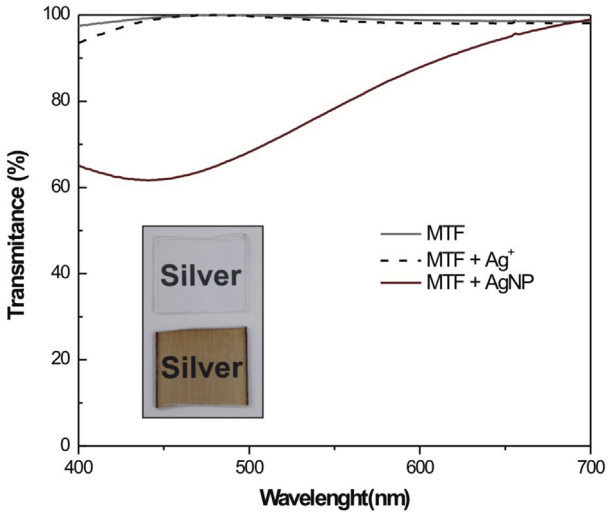

Fig. 3. Visible transmission spectra of control bilayer MTF coatings (grey curve), MTF coatings with adsorbed silver ions (black dashed curve) and MTF coatings with embedded silver nanoparticles (brown curve). Inset: picture of representative of glass slides with deposited MTF coatings denoting absolute optical transparency of MTF coatings loaded with silver ions (upper side). (For interpretation of the references to colour in this figure legend, the reader is referred to the web version of this article.)

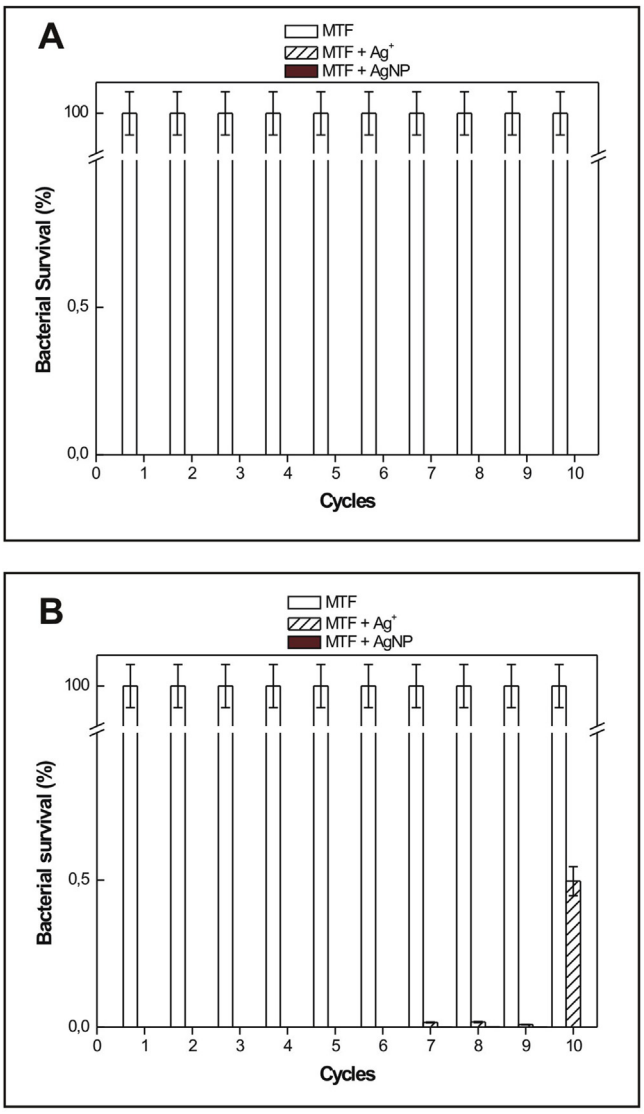

Fig. 4. Antibacterial activity of MTF coatings with adsorbed silver ions (white striped bars) and MTF coatings with embedded silver nanoparticles (brown bars) against *P. aeruginosa* (A) and *S. aureus* (B). Control bilayer MTF coatings are represented by white bars. Data are represented as mean ± SE (n = 3). For both strains, bacterial survival percentage in MTF + Ag^+ and in MTF + AgNP groups was significantly different from MTF in all cycles of use. (For interpretation of the references to colour in this figure legend, the reader is referred to the web version of this article.)

Staphylococcus aureus. In this case, there were no differences in the antimicrobial activity between MTF coatings until cycle 6. Indeed, from cycle 7 to 10 the R value was higher for MTF coatings loaded with silver nanoparticles than for MTF coatings loaded with silver ions. However, the R value was higher than 2.0 in all cases further confirming the effective antimicrobial activity (Table 2). These results confirm that MTF coatings loaded with silver ions exhibited a significant bactericidal long-term effect on *Pseudomonas aeruginosa* and *Staphylococcus aureus*, comparable to that observed with MTF coatings including silver nanoparticles. Moreover, it is worth to mention that the coating antibacterial functionality was retained even after 5 months from their synthesis, demonstrating their high stability under long-term storage.

Considering that MTF coatings loaded with silver ions offer the potentiality to function as devices that allow controlled release of silver ions for prolonged periods of time, the release of silver from both MTF coatings was analyzed over 10 cycles of use in the conditions at which antibacterial effects were tested. Silver mass release profile has shown to be similar between MTF coatings up to the 5th cycle of use. Thereafter, it has shown to be higher for MTF coatings loaded with silver nanoparticles. This observation suggests a slightly more sustained release of silver from that type of coatings, which could explain the differences in antibacterial efficiency observed between both MTF coatings only at last cycles of use. This profile showed a maximum of ca. 1.2 μg at cycle 2 followed by a slow decrease up to cycle 10, but not reaching a depletion of silver from coatings (Fig. 5A). As a result, cumulative release profile was similar to silver mass release profile (Fig. 5B), not reaching a plateau and confirming that after the tenth cycle of use MTF coatings were not significantly depleted from silver. This is an important observation as MTF coatings loaded with silver ions could have an extended bactericidal effect beyond the tenth cycle of use, similar to MTF coatings loaded with silver nanoparticles but offering a remarkable advantage over them: total optical transparency. In effect, curve fitting revealed that silver release followed a first-order kinetics with a half-time of 4.1 cycles and a $t_{90\%}$ (time at which 90% of silver load was released) of 13.2 cycles for MTF coatings loaded with silver ions, and a half-time of 6.9 cycles and a $t_{90\%}$ of 22.1 cycles for MTF coatings with embedded silver nanoparticles (Fig. 5B and Table 3).

Considering these findings and in order to estimate the remaining bactericidal effect of optically transparent MTF coatings, an isothermal adsorption experiment was performed by incubating MTFs with solutions of increasing $AgNO_3$ concentrations at 25 °C and monitoring the amount of remaining silver after 60 min exposure (Fig. 6). The best model to fit data was the Langmuir model, according to which silver ions electrostatically adsorb to the

Table 1
Coating antibacterial activity test results along 10 cycles of use for *Pseudomonas aeruginosa*.

Cycle of use	CFU[a] 0 h	MTF	MTF + Ag^+			MTF + AgNP		
		CFU 24 h	CFU 24 h	D[b]%	R[c]	CFU 24 h	D%	R
1	6.9×10^9	1.6×10^9	<10	>99.999	>8.19	<10	>99.999	>8.19
2	2.6×10^7	5.5×10^7	<10	>99.999	>6.74	<10	>99.999	>6.74
3	1.6×10^8	1.0×10^8	<10	>99.999	>7.01	<10	>99.999	>7.01
4	1.3×10^8	9.5×10^7	<10	>99.999	>6.98	<10	>99.999	>6.98
5	7.3×10^7	1.3×10^8	<10	>99.999	>7.10	<10	>99.999	>7.10
6	1.3×10^8	1.4×10^8	<10	>99.999	>7.16	<10	>99.999	>7.16
7	4.3×10^7	9.3×10^7	<10	>99.999	>6.97	<10	>99.999	>6.97
8	1.2×10^8	1.2×10^8	<10	>99.999	>7.09	<10	>99.999	>7.09
9	1.3×10^8	5.6×10^7	<10	>99.999	>6.75	<10	>99.999	>6.75
10	5.3×10^7	5.2×10^7	<10	>99.999	>6.71	<10	>99.999	>6.71

[a] CFU was calculated from the mean of 3 CFU counts.
[b] Percent reduction.
[c] Value of antimicrobial activity.

Table 2
Coating antibacterial activity test results along 10 cycles of use for *Staphylococcus aureus*.

Cycle of use	CFU 0 h	MTF	MTF + Ag^+			MTF + AgNP		
		CFU 24 h	CFU 24 h	D%	R	CFU 24 h	D%	R
1	4.3×10^5	1.1×10^5	<10	>99.999	>4.03	<10	>99.999	>4.03
2	1.5×10^8	1.5×10^6	<10	>99.999	>5.18	<10	>99.999	>5.18
3	3.0×10^4	2.2×10^3	<10	99.539	>2.34	<10	99.539	>2.34
4	1.8×10^8	3.9×10^8	<10	>99.999	>7.59	<10	>99.999	>7.59
5	1.2×10^8	1.8×10^9	<10	>99.999	>8.25	<10	>99.999	>8.25
6	4.3×10^8	3.0×10^7	<10	>99.999	>6.48	<10	>99.999	>6.48
7	1.4×10^{10}	3.0×10^{11}	4.8×10^7	99.984	3.79	2.0×10^5	>99.999	>6.17
8	3.1×10^6	1.6×10^7	2.8×10^3	99.983	3.76	1.2×10^2	>99.999	>5.12
9	2.8×10^8	2.3×10^8	2.0×10^4	99.991	4.05	6.0×10^2	>99.999	>5.58
10	1.1×10^6	1.6×10^6	7.9×10^3	99.504	2.30	<10	>99.999	>5.20

surface up to the formation of a homogenous monolayer. Once this monolayer is formed, it is reasonable that silver ions stop adsorbing on the mesoporous surfaces. The equilibrium adsorption constant (K_a) from the Langmuir fitting was 11.147 L mg^{-1}. Reported K_a for the adsorption of silver ions to different metal-oxide sorbents ranges from 0.006 to 3.740 L mg^{-1} [62–65]. The here reported higher K_a could be explained considering the extremely high surface area offered by the MTF coatings for silver ion adsorption. In addition, the maximum sorption capacity of film coatings was found to be ca. 3 μg of silver per cm^2, so that more than 15 μg of silver can be adsorbed onto each sample (5.2 cm^2). As the maximum cumulative amount of silver released from MTF coatings loaded with silver ions was less than 7 μg, this would imply that after 10 cycles of use, carried out over a period of 5 months, less than half of the amount of adsorbed silver was released. This stimulates the idea that their bactericidal effect could last much longer than 10 cycles of use. Even more, if we consider that MTF coatings were exposed to extremely high concentrations of bacteria, one could expect bactericidal effect with even much more perdurability in many real-life applications.

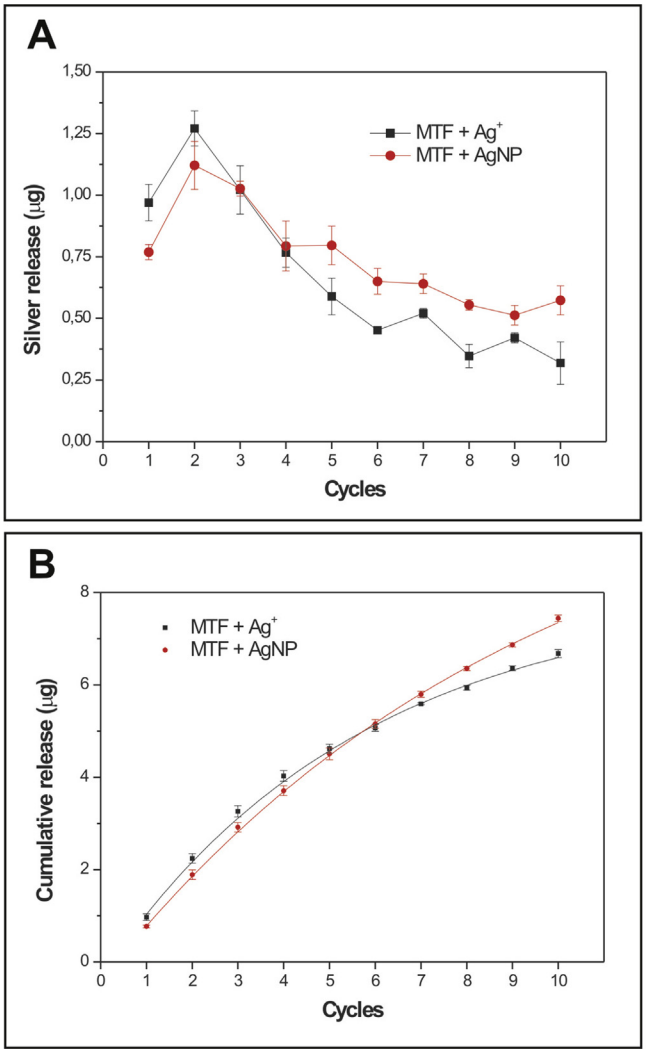

Fig. 5. Silver mass release (A) and cumulative release of silver (B) over 10 cycles of use of MTF coatings with adsorbed silver ions (black dots) and MTF coatings with embedded silver nanoparticles (red dots). Data are represented as mean ± SE (n = 3). Black and red lines indicate the result of experimental data fit using a first-order kinetics model. (For interpretation of the references to colour in this figure legend, the reader is referred to the web version of this article.)

Overall, in this study the bactericidal efficiency of two different silver ion-releasing systems was evaluated over time, demonstrating that optically transparent MTF coatings loaded only with silver ions offer high performance, comparable to MTF coatings loaded with silver nanoparticles. Beyond that an oxide bilayer MTF composition was selected as the basal structure for exclusively evaluating bactericidal effect of silver ions released from both MTF coating systems, based on the results, it would be expected that transparent coatings with long-term and highly efficient bactericidal activity can also be accomplished by oxide single layer MTF coatings in which the amount of loaded silver ions would depend on the total surface area offered by mesoporous reservoirs. That amount would ultimately define how long the antibacterial activity lasts.

Although a modest number of silver-doped transparent antibacterial coatings have been reported in the literature, by either using a layer-by-layer assembly of polyelectrolytes [66] or the sol-gel method to create organic–inorganic hybrid coatings [67,68], none of them demonstrated a long-lasting bactericidal effect as was described in this study. The presence of mesopores offering a very high number of silver ion adsorption sites, the chemical and mechanical stability of oxide matrices together with the possibility to obtain optically transparent nanometric thin film coatings with high and long lasting antibacterial activity, make the development of MTF coatings loaded with silver ions novel and unique.

4. Conclusions

Although there are previous reports on MTF coatings with silver-based antibacterial effect, these works always refer to the inclusion of silver nanoparticles within the coating. These nanoparticles exhibit a strong absorption in the range of visible light, which prevents those coatings to be transparent. In contrast, a

Table 3
First-order kinetics parameters for silver release from MTF coatings loaded with silver ions and silver nanoparticles.

Type of coating	k (min^{-1})	$t_{1/2}$ (cycles)	$t_{90\%}$ (cycles)	r^2
MTF + Ag^+	0.177	4.1	13.2	0.998
MTF + AgNP	0.106	6.9	22.1	0.999

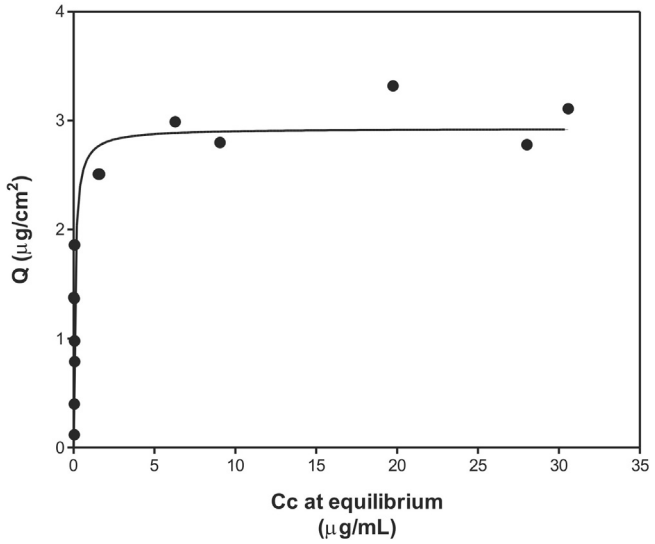

Fig. 6. Adsorption isotherm of silver on titania-silica bilayer MTF coating. The line indicates the result of experimental data fit using the Langmuir model.

mesoporous oxide thin film coating loaded with silver ions which exhibits optical transparency in the visible range and high long-lasting antibacterial activity is reported here for the first time. The mesopores, which offer high surface area, act as reservoirs of silver ions which, upon release, inhibit the growth of planktonic bacteria exposed to these coatings. In this way, it is possible to combat undesirable bacteria which can be transformed into a dangerous source of infection when are deposited on a surface. Even though the antibacterial MTF coating described here is based on a mesoporous titania-silica bilayer to the aim at exclusively evaluating bactericidal effect of silver ions released, this configuration offers flexibility, in the sense that single or multiple layers of mesoporous oxides could be deposited on a substrate in order to load different quantity of silver ions or other antibacterial agents. In addition, these coatings could be re-incubated with silver solution in order to prolong their bactericidal effect.

This transparent and colorless ceramic coating does not require any external activation and is inert, inexpensive, scalable and robust. Owing to all these advantages, it could be commercially applied in health centers and other places where the microbiological cleaning is needed, as in food processing facilities, playgrounds or dining. Although the biocompatibility of this silver loaded MTF coating will be determined in future studies, meanwhile, this MTF coating could be deposited onto ceramic surfaces such as sinks, baths or tiles and onto glass surfaces such as doors or windows, and on kitchen utensils. The coating could also be deposited on metal surfaces such as faucets and doorknobs, and medical equipment and instruments.

Acknowledgements

The authors thank Dr. L. Cerchietti and Dr. G. Custo for the determinations by X-ray fluorescence and for valuable discussions. This work was supported by grants from the Universidad de Buenos Aires UBACYT 20020150100056BA, from CONICET PIP 11220120100657CO and from Agencia Nacional de Promoción Científica y Tecnológica PICT 2012-1441 and 2012-2087. M.P. is grateful for her postdoctoral fellowship granted by CNEA. C.C. is member of CNEA. P.N.C., G. J. A. A. S-I, M.G.B. and M.F.D. are members of CONICET.

References

[1] J.W. Alexander, Surg. Infect. Larchmt 10 (2009) 289–292.
[2] A.B. Lansdown, Curr. Probl. Dermatol. 33 (2006) 17–34.
[3] S. Azlin-Hasim, M.C. Cruz-Romero, M.A. Morris, E. Cummins, J.P. Kerry, Food Packag. Shelf Life 4 (2015) 26–35.
[4] T.V. Duncan, J. Colloid Interface Sci. 363 (2011) 1–24.
[5] B. Nowack, H.F. Krug, M. Height, Environ. Sci. Technol. 45 (2011) 1177–1183.
[6] S.W.P. Wijnhoven, W.J.G.M. Peijnenburg, C.A. Herberts, W.I. Hagens, A.G. Oomen, E.H.W. Heugens, B. Roszek, J. Bisschops, I. Gosens, D. Van De Meent, S. Dekkers, W.H. De Jong, M. van Zijverden, A.J.A.M. Sips, R.E. Geertsma, Nanotoxicology 3 (2009) 109–138.
[7] J.W. Wiechers, N. Musee, J. Biomed. Nanotechnol. 6 (2010) 408–431.
[8] M.J. Carter, K. Tingley-Kelley, R.A. Warriner Iii, J. Am. Acad. Dermatol. 63 (2010) 668–679.
[9] M. Radulescu, E. Andronescu, G. Dolete, R.C. Popescu, O. Fufă, M.C. Chifiriuc, L. Mogoantă, T.-A. Bălşeanu, G.D. Mogoşanu, A.M. Grumezescu, Materials 9 (2016) 345.
[10] K. Vasilev, J. Cook, H.J. Griesser, Expert Rev. Med. Devices 6 (2009) 553–567.
[11] J. Hardes, H. Ahrens, C. Gebert, A. Streitbuerger, H. Buerger, M. Erren, A. Gunsel, C. Wedemeyer, G. Saxler, W. Winkelmann, G. Gosheger, Biomaterials 28 (2007) 2869–2875.
[12] D.W. Brett, Ostomy Wound Manag. 52 (2006) 34–41.
[13] S. Silver, A. Gupta, K. Matsui, J.-F. Lo, Met. Based Drugs 6 (1999) 315–320.
[14] Q.L. Feng, J. Wu, G.Q. Chen, F.Z. Cui, T.N. Kim, J.O. Kim, J. Biomed, Mater. Res. 52 (2000) 662–668.
[15] O. Choi, K.K. Deng, N.-J. Kim, L. Ross Jr., R.Y. Surampalli, Z. Hu, Water Res. 42 (2008) 3066–3074.
[16] C. Carlson, S.M. Hussain, A.M. Schrand, L.K. Braydich-Stolle, K.L. Hess, R.L. Jones, J.J. Schlager, J. Phys. Chem. B 112 (2008) 13608–13619.
[17] M.J. Piao, K.A. Kang, I.K. Lee, H.S. Kim, S. Kim, J.Y. Choi, J. Choi, J.W. Hyun, Toxicol. Lett. 201 (2011) 92–100.
[18] H.J. Park, J.Y. Kim, J. Kim, J.H. Lee, J.S. Hahn, M.B. Gu, J. Yoon, Water Res. 43 (2009) 1027–1032.
[19] D. Carmona, P. Lalueza, F. Balas, M. Arruebo, J. Santamaría, Microporous Mesoporous Mater. 161 (2012) 84–90.
[20] L. Ferreira, A.M. Fonseca, G. Botelho, C.A. Aguiar, I.C. Neves, Microporous Mesoporous Mater. 160 (2012) 126–132.
[21] W. Chen, Y. Liu, H.S. Courtney, M. Bettenga, C.M. Agrawal, J.D. Bumgardner, J.L. Ong, Biomaterials 27 (2006) 5512–5517.
[22] I. Noda, F. Miyaji, Y. Ando, H. Miyamoto, T. Shimazaki, Y. Yonekura, M. Miyazaki, M. Mawatari, T. Hotokebuchi, J. Biomed. Mater. Res. Part B 89B (2009) 456–465.
[23] S. Mandal, H.L. Williams, H.K. Hunt, Microporous Mesoporous Mater. 203 (2015) 245–258.
[24] G.S. Alvarez, C. Hélary, A.M. Mebert, X. Wang, T. Coradin, M.F. Desimone, J. Mater. Chem. B 2 (2014) 4660–4670.
[25] A.M. Mebert, C. Aimé, G.S. Alvarez, Y. Shi, S.A. Flor, S.E. Lucangioli, M.F. Desimone, T. Coradin, J. Mater. Chem. B 4 (2016) 3135–3144.
[26] M.L. Foglia, G.S. Alvarez, P.N. Catalano, A.M. Mebert, L.E. Diaz, T. Coradin, M.F. Desimone, Recent Pat. Biotechnol. 5 (2011) 54–61.
[27] M. Rai, S. Deshmukh, A. Ingle, A. Gade, J. Appl. Microbiol. 112 (2012) 841–852.
[28] V. D'Britto, H. Kapse, H. Babrekar, A. Prabhune, S. Bhoraskar, V. Premnath, B. Prasad, Nanoscale 3 (2011) 2957–2963.
[29] J. Liu, D.A. Sonshine, S. Shervani, R.H. Hurt, ACS Nano 4 (2010) 6903–6913.
[30] E.-R. Kenawy, S. Worley, R. Broughton, Biomacromolecules 8 (2007) 1359–1384.
[31] Y. Cong, T. Xia, M. Zou, Z. Li, B. Peng, D. Guo, Z. Deng, J. Mater. Chem. B 2 (2014) 3450–3461.
[32] M. Li, Q. Liu, Z. Jia, X. Xu, Y. Shi, Y. Cheng, Y. Zheng, J. Mater. Chem. B 3 (2015) 8796–8805.
[33] F. Tong, J. Gong, M. Li, C. Zeng, L. Zhang, Microporous Mesoporous Mater. 213 (2015) 1–7.
[34] M.S.L. Yee, P.S. Khiew, Y.F. Tan, W.S. Chiu, Y.Y. Kok, C.O. Leong, Microporous Mesoporous Mater. 218 (2015) 69–78.
[35] J.D. Oei, W.W. Zhao, L. Chu, M.N. DeSilva, A. Ghimire, H.R. Rawls, K. Whang, J. Biomed. Mater. Res. Part B 100 (2012) 409–415.
[36] Z. Shi, J. Tang, L. Chen, C. Yan, S. Tanvir, W.A. Anderson, R.M. Berry, K.C. Tam, J. Mater. Chem. B 3 (2015) 603–611.
[37] L. Guo, W. Yuan, Z. Lu, C.M. Li, Colloids Surf. A 439 (2013) 69–83.
[38] V. Ambrogi, A. Donnadio, D. Pietrella, L. Latterini, F.A. Proietti, F. Marmottini, G. Padeletti, S. Kaciulis, S. Giovagnoli, M. Ricci, J. Mater. Chem. B 2 (2014) 6054–6063.

[39] R. Cristescu, A. Visan, G. Socol, A.V. Surdu, A.E. Oprea, A.M. Grumezescu, M.C. Chifiriuc, R.D. Boehm, D. Yamaleyeva, M. Taylor, R.J. Narayan, D.B. Chrisey, Appl. Surf. Sci. 374 (2016) 290–296.
[40] Y.K. Jo, J.H. Seo, B.-H. Choi, B.J. Kim, H.H. Shin, B.H. Hwang, H.J. Cha, ACS Appl. Mater. Interfaces 6 (2014) 20242–20253.
[41] K.K. Goli, N. Gera, X. Liu, B.M. Rao, O.J. Rojas, J. Genzer, ACS Appl. Mater. Interfaces 5 (2013) 5298–5306.
[42] Y.I. Seo, Y.J. Lee, D.-G. Kim, K.H. Lee, Y. Do Kim, Microporous Mesoporous Mater. 139 (2011) 211–215.
[43] M.V. Roldán, P. de Oña, Y. Castro, A. Durán, P. Faccendini, C. Lagier, R. Grau, N.S. Pellegri, Mater. Sci. Eng. C 43 (2014) 630–640.
[44] Y. Liu, X. Wang, F. Yang, X. Yang, Microporous Mesoporous Mater. 114 (2008) 431–439.
[45] B. Yu, K.M. Leung, Q. Guo, W.M. Lau, J. Yang, Nanotechnology 22 (2011) 115603.
[46] A. Eremenko, A. Korduban, I. Gnatiuk, N. Vityuk, N. Smirnova, O. Linnik, Y. Mukha, Silver and gold nanoparticles on sol-gel TiO2, ZrO2, SiO2 surfaces: optical spectra, photocatalytic activity, bactericide properties, in: J. Cuppoletti (Ed.), Nanocomposites and Polymers with Analytical Methods, INTECH Open Access Publisher, Rijeka, Croatia, 2011, pp. 51–82.
[47] D.D. Evanoff, G. Chumanov, ChemPhysChem 6 (2005) 1221–1231.
[48] A. Taleb, C. Petit, M. Pileni, J. Phys. Chem. B 102 (1998) 2214–2220.
[49] E.L. Crepaldi, G.J.d.A. Soler-Illia, D. Grosso, F. Cagnol, F. Ribot, C. Sanchez, J. Am. Chem. Soc. 125 (2003) 9770–9786.
[50] R.I. Masel, Principles of Adsorption and Reaction on Solid Surfaces, John Wiley & Sons, New York, 1996.
[51] J.S. Association, JIS, (2000).
[52] E.D. Martínez, M.n.G. Bellino, G.J. Soler-Illia, ACS Appl. Mater. Interfaces 1 (2009) 746–749.
[53] J. Ginter, A. Kisielewska, K. Spilarewicz-Stanek, M. Cichomski, D. Batory, I. Piwoński, Microporous Mesoporous Mater. 225 (2016) 580–589.
[54] L. Rizzello, P.P. Pompa, Chem. Soc. Rev. 43 (2014) 1501–1518.
[55] L. Wei, J. Lu, H. Xu, A. Patel, Z.-S. Chen, G. Chen, Drug Discov. Today 20 (2015) 595–601.
[56] M.G. Bellino, S. Golbert, M.C. De Marzi, G.J.A.A. Soler-Illia, M.F. Desimone, Biomater. Sci. 1 (2013) 186–189.
[57] M. Kokunešoski, J. Gulicovski, B. Matović, M. Logar, S.K. Milonjić, B. Babić, Mater. Chem. Phys. 124 (2010) 1248–1252.
[58] M. Kosmulski, Chemical Properties of Material Surfaces, CRC press, New York, 2001.
[59] J.C. Yu, L. Zhang, Z. Zheng, J. Zhao, Chem. Mater. 15 (2003) 2280–2286.
[60] M. Zhou, J. Yu, H. Yu, J. Mol. Catal. A Chem. 313 (2009) 107–113.
[61] F. Borghi, V. Vyas, A. Podestà, P. Milani, PLoS One 8 (2013) e68655.
[62] H. Ghassabzadeh, A. Mohadespour, M. Torab-Mostaedi, P. Zaheri, M.G. Maragheh, H. Taheri, J. Hazard. Mater. 177 (2010) 950–955.
[63] P. Yin, Q. Xu, R. Qu, G. Zhao, J. Hazard. Mater. 169 (2009) 228–232.
[64] A. Sarı, M. Tüzen, Microporous Mesoporous Mater. 170 (2013) 155–163.
[65] L.-Y. Chai, S.-W. Wei, P. Bing, Z.-y. Li, Trans. Nonferr. Met. Soc. China 17 (2007) 832–835.
[66] X. Zan, Z. Su, Thin Solid Films 518 (2010) 5478–5482.
[67] S.M. Lee, B.S. Lee, T.G. Byun, K.C. Song, Colloids Surf. A 355 (2010) 167–171.
[68] P. Tatar, N. Kiraz, M. Asiltürk, F. Sayılkan, H. Sayılkan, E. Arpaç, J. Inorg. Organomet. Polym. Mater. 17 (2007) 525–533.